

# Left bundle branch block and echocardiography in the era of CRT

Yoshihiro Seo · Tomoko Ishizu · Fumiko Sakamaki ·  
Masayoshi Yamamoto · Kazutaka Aonuma

Received: 30 October 2014/Revised: 11 November 2014/Accepted: 11 November 2014/Published online: 26 November 2014  
© Japanese Society of Echocardiography 2014

**Abstract** Left ventricular (LV) dyssynchrony is a key pathophysiology in the era of cardiac resynchronization therapy (CRT). Left bundle branch block (LBBB) is the main substrate for CRT, and understanding the electrical pathophysiology is important in assessing the effects of CRT. Three-dimensional voltage mapping systems clearly demonstrate the typical propagation pattern characterized as propagation from the mid or apical septum to the lateral or posterior wall through the apex, which appears as a U shape. The electrical characteristics in LBBB closely associate with mechanical dyssynchrony, which is visualized as a septal flash motion. This rapid motion can be detected well by M-mode, tissue Doppler, and speckle tracking imaging. However, intraventricular discoordination between the septum and free wall is also a key to the response to CRT. We classified M-mode septum images into 10 patterns and septal strain pattern into two patterns. Through detailed analysis, we found that septal contraction contributes to intraventricular coordination. Therefore, in addition to septal flash, subsequent analysis of wall motion patterns also provides additional information about myocardial contractibility and the severity of electrical dyssynchrony. Recently, 3-dimensional speckle tracking imaging was introduced and used as a novel method to image electromechanical coupling. Because activation imaging by 3-dimensional speckle tracking can visualize similar U-shaped propagation images to those by

3-dimensional voltage mapping systems, it is hoped that this method will contribute to further research. Until now, it has not been fully understood how electrical dyssynchrony is expressed as mechanical abnormalities; therefore, continuous study will be required in the future.

**Keywords** Left bundle branch block · Dyssynchrony · Septal flash · M-mode imaging · Tissue Doppler imaging · Speckle tracking imaging

## Introduction

Assessments of left ventricular (LV) dyssynchrony have been the focus for over a decade and a half in the era of cardiac resynchronization therapy (CRT). Initially, CRT candidates were decided based only on the QRS duration. However, the latest update of the guidelines clearly states the superiority of the effects of CRT in left bundle branch block (LBBB)-type as compared with non-LBBB-type electrical disturbances [1]. However, even in LBBB, some candidates for CRT may be non-responders, and, therefore, improvements in echocardiographic methods still have clinical implications in the prediction of CRT responders. In this review article, we focus on the association between electrical dyssynchrony and its mechanical expressions on Doppler echocardiographic images in LBBB.

## Intraventricular electrical conduction and muscle activation

Normal pattern

Tawara [2] carried out a formidable study lasting over 2 years that was based on reconstructing the conduction

Y. Seo (✉) · T. Ishizu · M. Yamamoto · K. Aonuma  
Cardiovascular Division, Faculty of Medicine, University of  
Tsukuba, 1-1-1 Tennodai, Tsukuba 305-8575, Japan  
e-mail: yo-seo@md.tsukuba.ac.jp

F. Sakamaki  
Clinical Laboratory, University of Tsukuba Hospital, Tsukuba,  
Japan

system from serial sections. The extensive branching of the Purkinje fibers makes studies of this kind extremely difficult. Normal activation of the ventricles starts with conduction of the electrical impulse from the atrioventricular node to the His bundle. The His bundle splits into the right and left bundle branches, which divide first into a few major branches (fascicles) and subsequently into a network of subendocardially located Purkinje fibers (Fig. 1a) [3–5]. The septal portion of the network of Purkinje fibers does not contribute to the activation of ventricular muscle until it reaches approximately the junction between the middle and lower third of the septum (Fig. 1b). At this site, initial muscle depolarization occurs, and the wave front is reversed and propagates to the upper two-thirds of the septum from the apex to the base, traveling through muscle instead of conducting tissue. Simultaneously, the conduction system over the lower third of the septum is conducting the impulse toward the apex, with the neighboring muscle following closely in the wake of conduction system activation, and in the same direction. In the free wall, the conducting tissue from the two divisions of the bundle branch appears to merge. This ring of conducting tissue formed by the merger of the two major divisions joins a free-wall subendocardial network. The septal network of

conducting tissue, after passing across the lower septum and apex, ascends the free wall in the interpapillary region, activating the muscle mass en route. This network makes muscle activation propagate from the apex to the base in both the free wall and in the septum.

### Septal conduction in LBBB

In patients with complete LBBB, electrical activation must proceed through the interventricular septum from the right ventricular endocardium to the LV endocardium [6–8]. The septal conduction requires more than 40 ms in complete LBBB, which indicates a cell-to-cell propagation from the right to left ventricle but not via a conduction system like the Purkinje fibers (Fig. 2) [7, 8]. The first activation site of the LV endocardium is termed the breakthrough site, which is a single site located in the mid to apical septum. In contrast, subtype conductions have been reported even in LBBB on conventional ECGs. Such patients have multiple breakthrough sites at the LV basal region in addition to the mid to apical septum and have a normal septal conduction time. In this pattern, a residual conduction system from the right to left ventricle is suggested; namely, these patients do not actually have complete LBBB.

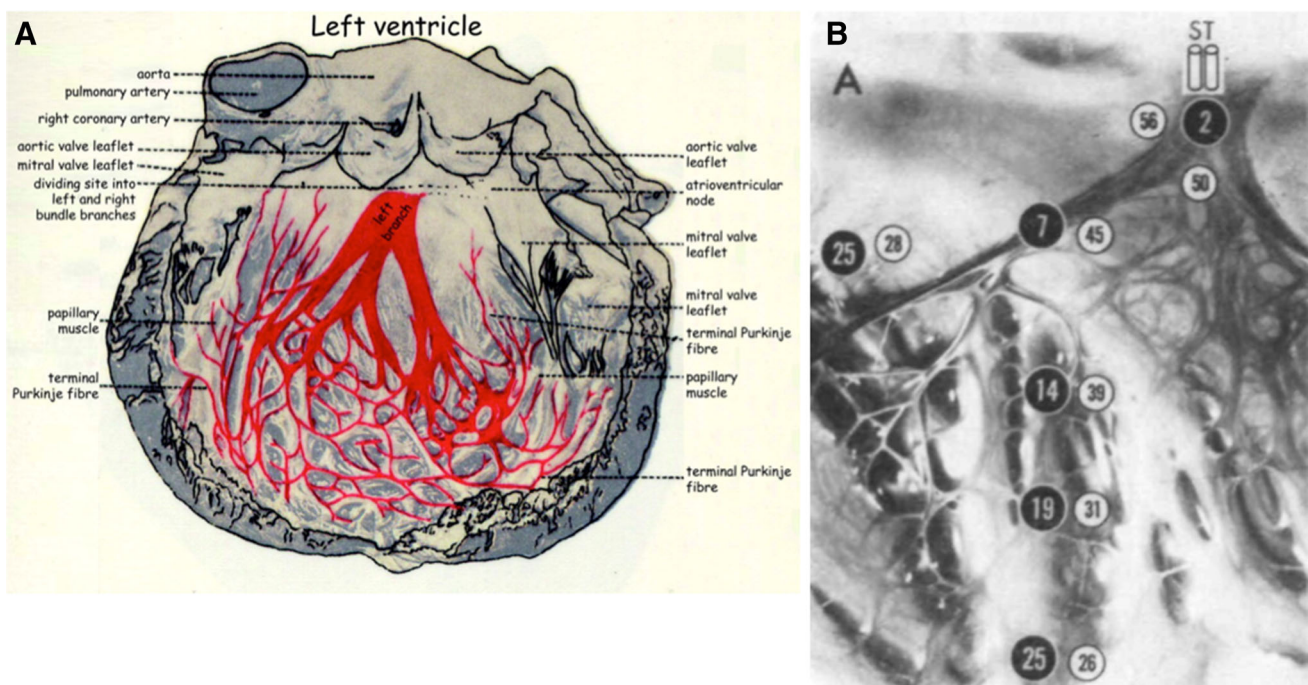
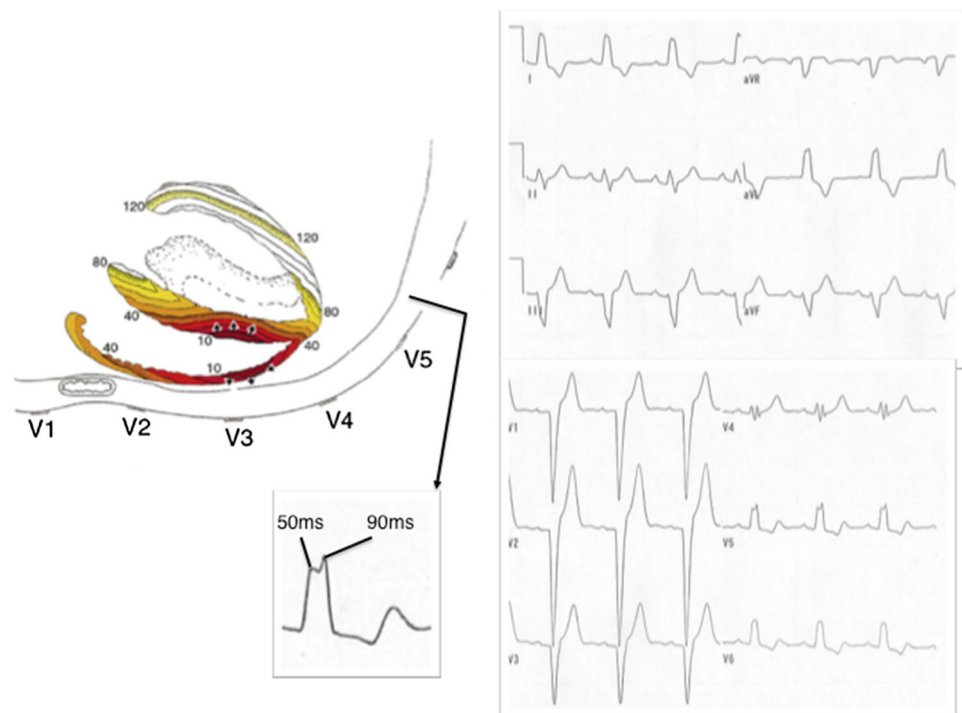


**Fig. 1 a** The His–Purkinje system in the human left ventricle modified from Tawara [2] adapted from Boyett [4]. **b** Normal sequence of activation of the left bundle branch system and left ventricular endocardium. Activity is propagated from the top of the septum toward the apex through conducting tissue. The conduction time from the main bundle branch to the conducting tissue in the lower third of the septum is generally in the range of 16–25 ms, which

is indicated by *white numbers in black circles* for conducting tissue. The activation time of ordinary ventricular muscle is progressively higher in the septum, it becomes progressively later, and the interval between septal Purkinje activity and septal muscle activity is prolonged, which is indicated by the *black numbers in white circles* for ordinary muscle. ST, stimulation site. Adopted from Myerburg et al. [5]

**Fig. 2** Left bundle branch block (LBBB) activation sequence and representative QRS-T waveforms are depicted in their anatomic locations for the transverse plane. The key LBBB QRS morphology feature shown is the mid-QRS notching that occurs at 50 and 90 ms, with slurring in between. The *first notch* represents the time when the electrical depolarization wave front reaches the endocardium of the left ventricle (after proceeding through the septum). The *second notch* occurs when the depolarization wave front begins to reach the epicardium of the posterolateral wall. Modified from Strauss et al. [7]



### Intraventricular conduction in LBBB

In patients with LBBB, the total LV endocardial activation time ranges from 60 to 160 ms. However, using 3-dimensional endocardial mapping systems, Auricchio et al. [8] reported that etiology does not seem to have a major effect on the total endocardial activation time. The characteristic propagation pattern is that of propagation from the mid or apical septum to the lateral or posterior wall through the apex, which appears as a U shape. The activation does not directly propagate from the septum to the lateral wall through the anterior wall, indicating the presence of a line of block (Fig. 3). The location of this line of block varies and includes locations in the anterior, lateral, or inferior wall. However, the line of block is located in the anterior wall in patients with an apical septal breakthrough site, which means a larger degree of electrical disarrangement between the two ventricles and within the left ventricle as compared to patients with the line of block in the lateral wall.

### Definition of complete LBBB by ECG

Based on the electrical activation sequence mentioned above, a minimum threshold to diagnose complete LBBB is more than 140 ms in men and 130 ms in women because LV electrical depolarization is delayed by more than 40 ms while passing through the septum and is then delayed by an additional 20–40 ms beyond

the normal conduction time as it reaches the posterolateral wall. In addition, a QS or rS pattern in leads V1 and V2 and mid-QRS notching or slurring in more than two of leads V1, V2, V5, V6, I, and aVL are needed (Fig. 2) [7].

### Echocardiography in LBBB

#### B-mode imaging

The septal motion in LBBB depends on the interaction of electrical propagation and pressure between both ventricles. Based on the electrical propagation pattern in LBBB, septal contraction ought to be generated first or, at least, be generated faster than LV free-wall contraction. The early motion of the systolic wall has been called septal flash motion, which is a representative wall motion in LBBB. The septal flash can be observed as a septal motion inward toward the left ventricle, followed by a counter motion toward the right ventricle during early systole, including the isovolumic systolic phase (Fig. 4a). This interaction between the septal wall and free wall causes apical shuffle, which can be visualized in an apical four-chamber view (Fig. 4a). As mentioned earlier, the electrical activation in LBBB propagates from the mid or apical septum to the lateral or posterior wall through the apex. Septal flash motion strongly correlates with this U-shaped electrical propagation pattern [9].

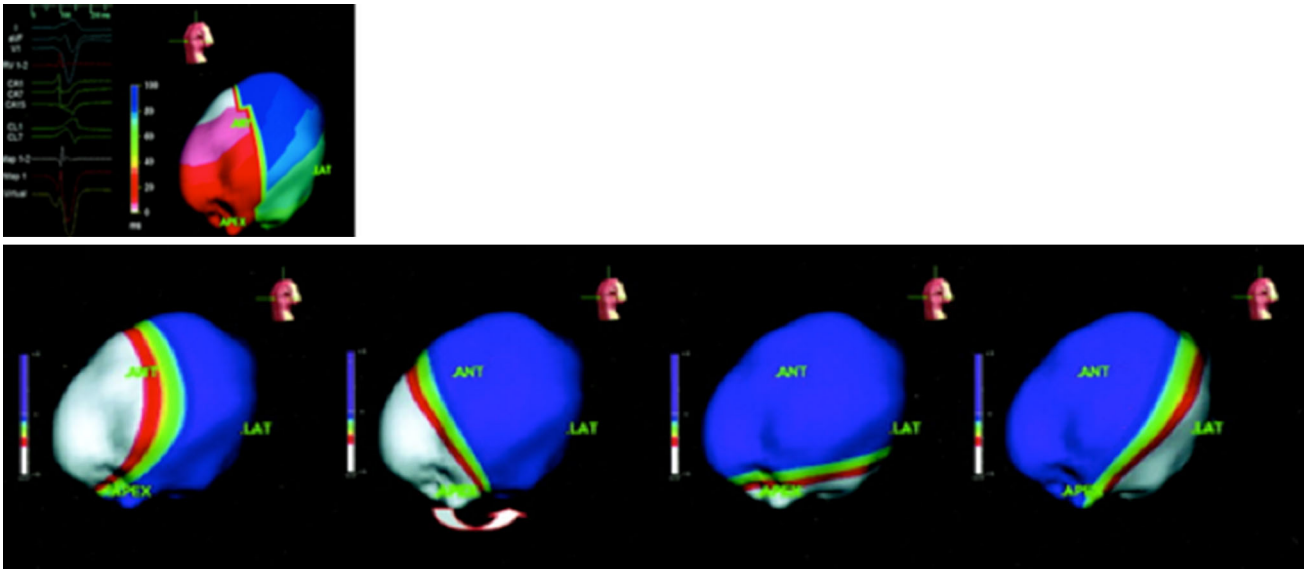


**Fig. 3** U-shaped propagation pattern in LBBB shown by a voltage mapping system. Adapted from Auricchio et al. [8]

Septal flash motion was previously thought to be a passive motion caused by the pressure gradient between the right and left ventricles, because the right ventricle is activated earlier than the left ventricle in LBBB [10]. However, subsequent studies revealed that septal flash is caused by active septal contraction [8, 11]. Because the LV free wall is still not activated in LBBB during early systole, LV pressure does not increase rapidly, and, thus, the septum can contract due to the reduced afterload against it. Subsequently, septal inward motion is suddenly stopped, which is caused for two reasons. First, the timing of septal motion stop corresponds to the timing of complete mitral valve closing, which means that septal contraction stop may be caused by the arrest of a change in LV volume. Second, increased LV pressure by contraction of the free wall may also cause septal motion to stop. A subsequent counter wall motion toward the right ventricle is mainly caused by the increasing LV pressure. Because the septal wall cannot generate wall stress against the increased LV pressure, the septal wall is pushed back toward the right ventricle, which looks like dyskinesia, even if the septal wall continues to contract.

Septal wall motion after septal flash varies. In a patient with preserved free wall contraction, septal wall motion depends on its contractibility and timing of the free-wall contraction. In a patient with a certain level of preserved septal contractibility, a second motion toward the left ventricle may be observed after equalization of the wall stress between the septum and free wall during the ejection phase. In contrast, in a patient with reduced septal contractibility, the septum may continue its dyskinetic motion

because it cannot generate adequate wall stress. The reason for this may be due to remodeling with reduced myocardial mass. In addition, septal contraction might be finished before the onset of free-wall contraction due to markedly delayed activation.

If free-wall contractibility is deteriorated, septal contraction may be prolonged, which does not look like septal flash because the free wall cannot generate wall stress against the septum to stop septal inward motion and push back toward the right ventricle (Fig. 4b). In such a case, mechanical dyssynchrony between the septum and wall motion may be counterbalanced.

#### M-mode imaging

M-mode imaging is a classic method of assessing LV dyssynchrony. It is clinically attractive because it is a fundamental function that is included in all echocardiographic systems. As mentioned in the B-mode imaging section earlier, septal flash is a key observation in LBBB; however, this rapid and small wall motion cannot be tracked by eyeball evaluation in all cases. Thus, M-mode imaging with its high time resolutions may be useful in assessing dyssynchrony in LBBB. However, the available scanning area of M-mode imaging is limited in the septum and posterolateral wall. Recently, we confirmed that standard M-mode imaging has limitations in visualizing septal flash, despite its higher temporal resolution [12]. In contrast, anatomical M-mode is useful to visualize early septal displacements. In one half of the cases with no apparent early septal displacement by standard M-mode imaging, the septal displacement could be newly visualized if the

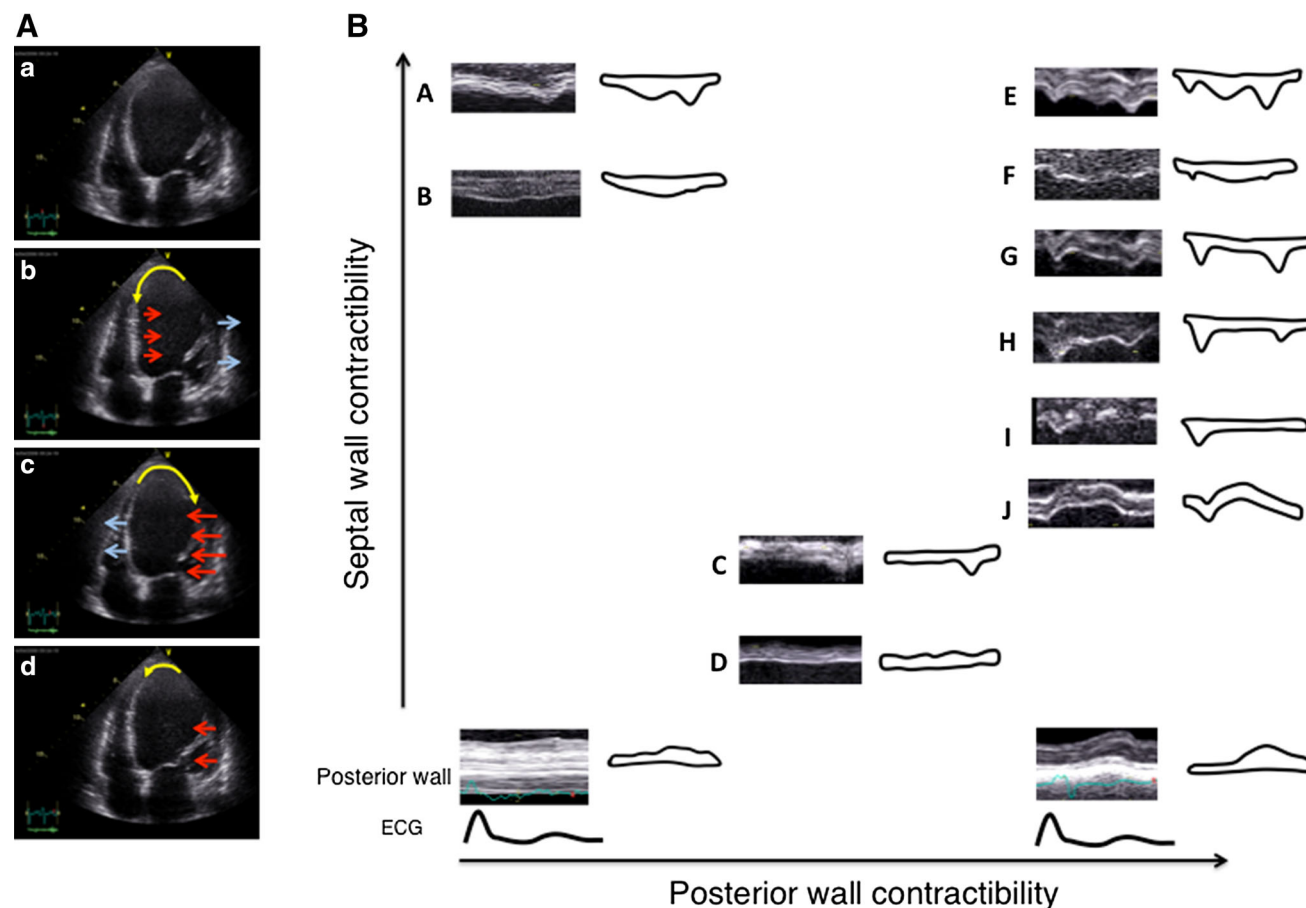


**Fig. 4** **a** Septal flash and apical shuffle motion in LBBB. *Panel A* A four-chamber image at end-diastole in a patient with idiopathic dilated cardiomyopathy. *Panel B* Septal inward motion (red arrows) and accompanying outward motion in the lateral wall (blue arrows) in the pre-ejection phase. The yellow arrow indicates the apical rotation of apical shuffle. *Panel C* Septal counter motion toward the right ventricle (blue arrows) and lateral wall contraction at the mid-ejection phase. *Panel D* Prolonged lateral wall contraction at the post-systolic phase. **b** Classifications of M-mode images based on both septal and posterior wall contractibility. The details are summarized in the text. **c** Tissue Doppler-derived velocity–time curves of the septum and lateral wall. Basal and mid septal wall motion are shown by the yellow and blue curves, and basal and mid lateral motion are shown by the red and green curves, respectively. The peak positive velocity component as active wall motion is indicated by a downward arrow and as passive wall motion by an upward arrow. The first active septal motion is present at the pre-ejection phase between mitral valve closing (MVC) and aortic valve opening (AVO). In contrast, the first lateral wall motion is passive, which corresponds to the outward motion in the lateral wall, as shown in Fig. 4b, *Panel B*.

scan area was spread at the inferoseptal area using anatomical M-mode.

We classified septal M-mode images into 10 patterns in patients with LBBB (Fig. 4b) [12]. The classifications are based on the relation between septal and posterior wall contractibility. There is an early septal wall motion in patterns E to J, which corresponds to

Subsequently, the septal peak velocity in the ejection phase between AVO and aortic valve closing (AVC) is a second active wall motion, which may correspond to the second peak, as shown in Fig. 4b, pattern E. Based on the electrical sequence of LBBB, the time interval between the first septal peak in the pre-ejection phase and the first active lateral wall motion in the ejection phase may indicate adequate mechanical dyssynchrony. ECG electrocardiogram. Modified from Sakamaki et al. [21]. **d** Speckle tracking imaging in LBBB. *Panels A* (pattern A) and *B* (pattern B) show radial strain–time curves in patients with LBBB and idiopathic dilated cardiomyopathy, respectively. Pattern A is characterized by an anteroseptal curve (yellow curve) with positive strain and subsequent negative strain. The purple curve shows a posterior wall curve. In pattern B, the anteroseptal curve (yellow curve) shows continuous positive strain. In the comparisons between groups,  $+dP/dt$  by high-fidelity, micromanometer-tipped catheter was significantly higher in pattern B compared to pattern A, which means that septal contraction contributes to maintaining intraventricular coordination (*bottom panel*). Pattern A may correspond to pattern J in Fig. 4b, and pattern B may correspond to pattern E. Unpublished data by Seo

septal flash. In patterns E to H, a second inward motion is observed during the mid-ejection phase, which means that the septum may continue to contract against increased wall stress. In contrast, early septal wall motion cannot be observed in patterns A and B, in which posterior wall contraction is markedly reduced. Because of the reduced counter stress by the free wall

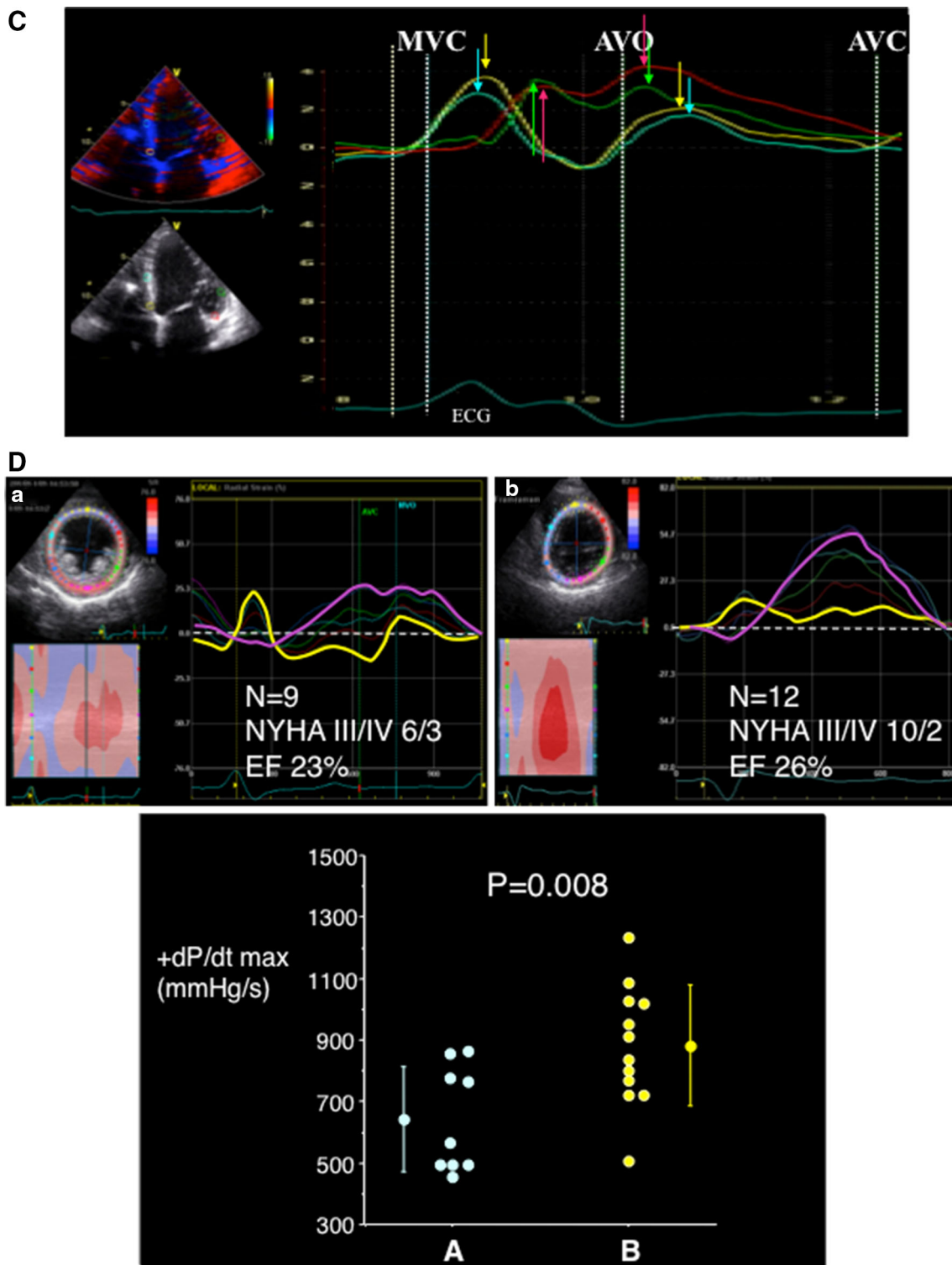


Fig. 4 continued

in these cases, early septal wall motions are prolonged until the mid-ejection phase. In patterns C and D, dyssynchrony analysis is unavailable because septal contractibility is markedly reduced.

Tissue Doppler imaging

Tissue Doppler imaging (TDI) had been a superstar in assessing LV dyssynchrony [13–16]. However, multicenter

studies including the Predictors of Response to CRT (PROSPECT) trial and the Japan Cardiac Resynchronization Therapy Registry Trial (J-CRT) showed negative results in terms of the utility of TDI in identifying CRT responders [17, 18]. LV dyssynchrony with TDI has been assessed by myocardial velocity–time curves, and almost all TDI-derived dyssynchrony parameters defined for measurement are restricted to the ejection period [13–16]. Because myocardial velocity–time curves have multiple and various peaks throughout the systolic phase that cause confusion when selecting the appropriate peaks (Fig. 4c), limitation of the phase to the ejection period may simplify dyssynchrony assessments.

However, septal early active wall motion, namely septal flash, may be present during the pre-ejection period in LBBB, as previously mentioned. We confirmed that a peak velocity derived from the first active septal wall motion was observed during the pre-ejection period in almost all patients with LBBB [19]. Therefore, in addition to M-mode imaging, TDI should also be used to identify septal flash motion [20, 21].

#### 2D-Speckle tracking imaging

Speckle tracking echocardiography (STE), a novel technique using B-mode echocardiographic images, has been developed as a reliable modality to assess regional LV deformation [22, 23]. STE can provide 3 components of LV deformation, including radial strain, circumferential strain, and longitudinal strain.

In LBBB, the strain–time curves clearly demonstrate regional dyssynchronous motions (Fig. 4d). In the septal strain–time curves, early septal deformation, which corresponds to septal flash, and subsequent septal kinetics are visualized more than with M-mode imaging. In contrast, early stretch and subsequent delayed and prolonged contraction also are visualized. In particular, discoordination between the septum and free wall can be confirmed as described in the M-mode imaging section. Note the marked similarities between the M-mode images and STE-derived strain–time curves. The discoordination can be easily confirmed by STE; however, a method for quantification has not yet been established. As well as in M-mode septal images (Fig. 4b), septal contractibility may also be estimated by the strain–time curve pattern (Fig. 4d), and preserved septal contractibility may indicate preservation of global LV systolic function.

#### 3D-Speckle tracking imaging

The advent of three-dimensional echocardiography represents a major innovation in cardiovascular ultrasound [24].

Because electromechanical coupling-based dyssynchrony imaging may be useful in assessing intraventricular dyssynchrony, we introduced novel three-dimensional speckle tracking echocardiography (3D-STE) software to visualize mechanical activation (activation imaging) [25]. Because previous studies with voltage mapping systems demonstrated various propagation patterns even in patients with LBBB [8, 26], 3D-STE-derived activation imaging is modeled after 3D voltage mapping systems. In patients with LBBB, the main activation pattern appears as a U shape (Fig. 5). The activation does not directly propagate from the septum to the lateral wall through the anterior wall. This pattern is quite similar to that of voltage mapping images (Fig. 3). In particular, septal flash was observed in almost all patients with this propagation pattern. In a second pattern, although the initial activation segments are present in the septum, the propagation block and the U shape are not present, and activation is diffusely propagated into the free wall. In addition, a third pattern shows marked regional conduction delay in the free wall. Regions with markedly delayed onset of contraction might suggest the presence of scar or less viable myocardium, rather than electrical dyssynchrony.

#### Role of echocardiography to predict CRT response in LBBB

The latest update to the guidelines clearly states the superiority of the effects of CRT in LBBB-type as compared with non-LBBB-type electrical disturbances [1]. However, even in LBBB, some candidates for CRT may be non-responders, which are defined as patients in whom the LV end-systolic volume reduction is less than 15 %. Therefore, improvements of echocardiographic methods still have clinical implications in the prediction of CRT responders [27]. In our experience, 27 % of patients with LBBB who received CRT were non-responders [18].

As shown in Fig. 4b, mechanical dyssynchrony varies depending on myocardial contractibility and the propagation pattern of electrical activation, even in similar LBBB patterns on the ECG. Through this review, the reader must have noticed that septal flash is the key to mechanical dyssynchrony in LBBB. Septal flash has a strong association with the typical U-shaped electrical propagation pattern, which is the best substrate for response to CRT. Therefore, septal flash should be confirmed at first not only by eyeball assessment but also by M-mode imaging, TDI, and STE. The most important thing is to evaluate early systolic septal motion instead of septal motion during the ejection or post-systolic phase [12, 21, 28]. In addition, mechanical discoordination should be evaluated after septal flash assessments. The M-mode pattern or strain curve

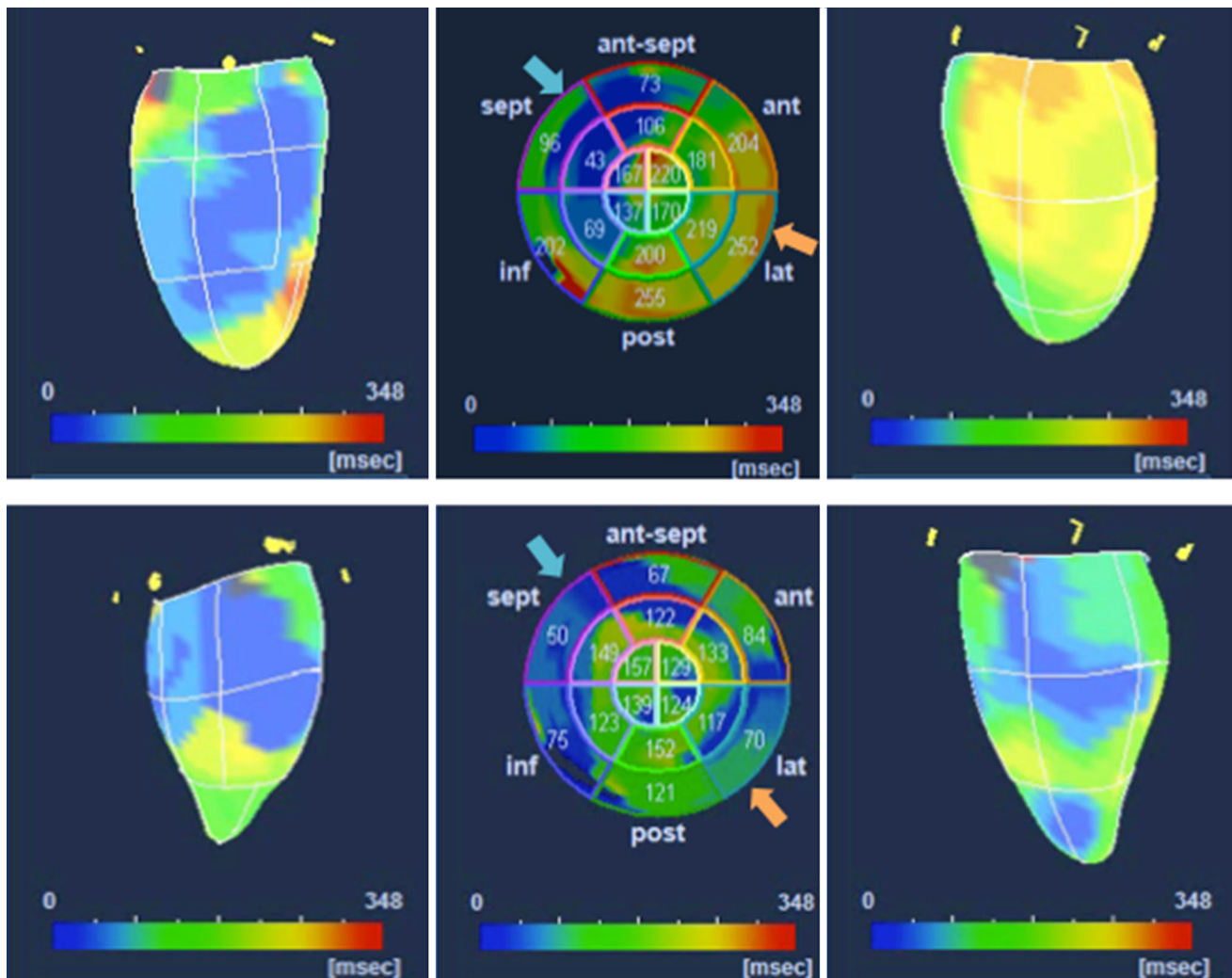


**Fig. 5** Changes in activation imaging by cardiac resynchronization therapy (CRT). The *center panels* show baseline (*upper*) activation imaging and that after CRT (*lower*). The *left panels* show 3-dimensional activation imaging as seen from the direction of the septal wall (*blue arrows* in the *center panels*). The *right panels* are as seen from

the direction of the lateral wall (*orange arrows* in the *center panels*). This case shows the typical U-shaped propagation pattern before CRT. After CRT, the free walls were colored *blue* or *green*, which indicates resynchronization. Adopted from Seo et al. [28]

analysis can provide additional information about the nature of the myocardium (Figs. 2 and 4a).

**Conclusion**

Doppler echocardiography has become a promising tool in the assessment of left ventricular (LV) dyssynchrony in left bundle branch block (LBBB). However, it has not been fully understood how electrical dyssynchrony is expressed as mechanical abnormalities; therefore, continuous study will be required in the future.

**Conflict of interest** Yoshihiro Seo, Tomoko Ishizu, Fumiko Sakamaki, Masayoshi Yamamoto, and Kazutaka Aonuma declare that they have no conflict of interest.

**References**

1. Epstein AE, DiMarco JP, Ellenbogen KA, et al. 2012 ACCF/AHA/HRS focused update incorporated into the ACCF/AHA/HRS 2008 guidelines for device-based therapy of cardiac rhythm abnormalities: a report of the American College of Cardiology Foundation/American Heart Association Task Force on Practice Guidelines and the Heart Rhythm Society. *J Am Coll Cardiol.* 2013;61:e6–75.
2. Tawara S. Das Reizleitungssystem des Säugetierherzens. Eine anatomisch–histologische Studie über das Atrioventricularbündel und die Purkinjeschen Fäden. Jena, Gustav Fischer, 1906. (Tawara S. The conduction system of the mammalian heart. Suma K, Shimada M, trans. London, UK: Imperial College Press, 2000).
3. Ansari A, Ho SY, Anderson RH. Distribution of the Purkinje fibres in the sheep heart. *Anat Rec.* 1999;254:92–7.
4. Boyett MR. ‘And the beat goes on.’ The cardiac conduction system: the wiring system of the heart. *Exp Physiol.* 2009;94: 1035–49.



5. Myerburg RJ, Nilsson K, Gelband H. Physiology of canine intraventricular conduction and endocardial excitation. *Circ Res*. 1972;30:217–43.
6. Vassallo JA, Cassidy DM, Marchlinski FE, et al. Endocardial activation of left bundle branch block. *Circulation*. 1984;69: 914–23.
7. Strauss DG, Selvester RH, Wagner GS. Defining left bundle branch block in the era of cardiac resynchronization therapy. *Am J Cardiol*. 2011;107:927–34.
8. Auricchio A, Fantoni C, Regoli F, et al. Characterization of left ventricular activation in patients with heart failure and left bundle-branch block. *Circulation*. 2004;109:1133–9.
9. Duckett SG, Camara O, Ginks MR, et al. Relationship between endocardial activation sequences defined by high-density mapping to early septal contraction (septal flash) in patients with left bundle branch block undergoing cardiac resynchronization therapy. *Europace*. 2012;14:99–106.
10. Little WC, Reeves RC, Arciniegas J, et al. Mechanism of abnormal interventricular septal motion during delayed left ventricular activation. *Circulation*. 1982;65:1486–91.
11. Leenders GE, Lumens J, Cramer MJ, et al. Septal deformation patterns delineate mechanical dyssynchrony and regional differences in contractility: analysis of patient data using a computer model. *Circ Heart Fail*. 2012;5:87–96.
12. Sakamaki F, Seo Y, Atsumi A, et al. Novel dyssynchrony evaluation by M-mode imaging in left bundle branch block and the application to predict responses for cardiac resynchronization therapy. *J Cardiol*. 2014;64:199–206.
13. Sogaard P, Egeblad H, Kim WY, et al. Tissue Doppler imaging predicts improved systolic performance and reversed left ventricular remodeling during long-term cardiac resynchronization therapy. *J Am Coll Cardiol*. 2002;40:723–30.
14. Gorcsan J 3rd, Kanzaki H, Bazaz R, et al. Usefulness of echocardiographic tissue synchronization imaging to predict acute response to cardiac resynchronization therapy. *Am J Cardiol*. 2004;93:1178–81.
15. Yu CM, Zhang Q, Fung JW, et al. A novel tool to assess systolic asynchrony and identify responders of cardiac resynchronization therapy by tissue synchronization imaging. *J Am Coll Cardiol*. 2005;45:677–84.
16. Bax JJ, Bleeker GB, Marwick TH et al. Left ventricular dyssynchrony predicts response and prognosis after cardiac resynchronization therapy. *J Am Coll Cardiol*. 2004;44:1834–40.
17. Chung ES, Leon AR, Tavazzi L, et al. Results of the predictors of response to CRT (PROSPECT) trial. *Circulation*. 2008;117: 2608–16.
18. Seo Y, Ito H, Nakatani S, et al. The role of echocardiography in predicting responders to cardiac resynchronization therapy: results from the Japan cardiac resynchronization therapy registry trial (J-CRT). *Circ J*. 2011;75:1156–63.
19. Seo Y, Ishizu T, Sakamaki F, et al. Analysis of the origin of cardiac wall motion that constitutes myocardial velocity–time curves in patients with left bundle branch block. *J Am Soc Echocardiogr*. 2009;22:331–6.
20. Miyazaki C, Lin G, Powell BD, et al. Strain dyssynchrony index correlates with improvement in left ventricular volume after cardiac resynchronization therapy better than tissue velocity dyssynchrony indexes. *Circ Cardiovasc Imaging*. 2008;1:14–22.
21. Sakamaki F, Seo Y, Ishizu T, et al. Tissue Doppler imaging dyssynchrony parameter derived from the myocardial active wall motion improves prediction of responders for cardiac resynchronization therapy. *Circ J*. 2012;76:689–97.
22. Amundsen BH, Helle-Valle T, Edvardsen T, et al. Noninvasive myocardial strain measurement by speckle tracking echocardiography: validation against sonomicrometry and tagged magnetic resonance imaging. *J Am Coll Cardiol*. 2006;47:789–93.
23. Korinek J, Kjaergaard J, Sengupta PP, et al. High spatial resolution speckle tracking improves accuracy of 2-dimensional strain measurements: an update on a new method in functional echocardiography. *J Am Soc Echocardiogr*. 2007;20:165–70.
24. Kwan J. Three-dimensional echocardiography: a new paradigm shift. *J Echocardiogr*. 2014;12:1–11.
25. Seo Y, Yamasaki H, Kawamura R, et al. Left ventricular activation imaging by 3-dimensional speckle-tracking echocardiography. Comparison with electrical activation mapping. *Circ J*. 2013;77:2481–9.
26. Fung JW, Chan JY, Yip GW, et al. Effect of left ventricular endocardial activation pattern on echocardiographic and clinical response to cardiac resynchronization therapy. *Heart*. 2007;93:432–7.
27. Sipahi I, Chou JC, Hyden M, et al. Effect of QRS morphology on clinical event reduction with cardiac resynchronization therapy: meta-analysis of randomized controlled trials. *Am Heart J*. 2012;163:260–7.
28. Seo Y, Ishizu T, Sakamaki F, et al. Mechanical dyssynchrony assessed by speckle tracking imaging as a reliable predictor of acute and chronic response to cardiac resynchronization therapy. *J Am Soc Echocardiogr*. 2009;22:839–46.